An integrated petrophysical analysis based on NMR, organic geochemistry and mineralogy. The Vaca Muerta source rock-unconventional play at different thermal maturities

Diana Masiero[1*], *Marcos* Comerio[1], *Esteban* Domené[1], *Gabriela* Vila[1], *Bernarda* Epele[1], *Mariano* Cipollone[1], *Mariela* Silka[2], *Carlos* Camacho[3], *Lourdes* Vera López[2] and *Silvina* Chiappero[2]

[1]YPF-Tecnología S.A. (Y-TEC-CONICET), Buenos Aires, Argentina
[2]YPF S.A., Buenos Aires, Argentina
[3]EQUINOR ASA, Houston, TX, United States of America

Abstract. The Vaca Muerta Formation (Upper Jurassic–Lower Cretaceous) of the Neuquén Basin, Argentina is a world-class source rock and renowned as an unconventional reservoir for both oil and gas. The present study examines rotary sidewall cores representative of the oil and gas windows to analyze correlations between nuclear magnetic resonance (NMR T_2 and T_1-T_2 maps at 2 MHz), Gas Filled Porosity (GFP), Rock-Eval programmed pyrolysis and quantitative X-ray diffraction (XRD) mineralogy. Shale samples are characterized by high present-day total organic carbon contents ranging from 3 to 7.20% (mean: 4.30%) for Well A at the oil window and, 0.72 to 11.77% (mean: 5.86%) for Well B at the gas window. The analyzed set also covers a wide compositional spectrum from carbonate-rich (> 50% of calcite and minor dolomite), mixed carbonate-siliciclastic (30 to 50% of calcite), to siliciclastic-rich (< 30% of calcite) samples. Notably, the clay fraction is dominated by interstratified illite-smectite minerals with less than 10% of expandable layers. Total porosity, calculated from Gas Filled Porosity plus NMR T_2 Cumulative Distribution, is in the range of 10 to 20 porosity units. In this work we also present a new NMR sequence to detect solid-like organic matter with NMR at 2 MHz in an integrated workflow to characterize petrophysical properties of the Vaca Muerta Formation.

1 Introduction

Petrophysical studies are envisioned to characterize both conventional and unconventional reservoirs based on the evaluation of different properties including lithology, wettability, fluid saturation and composition, as well as porosity and permeability [1, 2]. Contrary to conventional reservoirs, a complete petrophysical analysis of unconventional plays, in particular shale rocks characterized by fine-grained components, presence of organic matter, and heterogenous lithologies is still challenging and new case studies are needed to obtain different workflow strategies.

The Vaca Muerta Formation of the Neuquén Basin Argentina, is a marine source rock with excellent characteristics from the perspective of source rock-unconventional plays: (1) high present-day TOC content (1 – 8% with peaks of 12%); (2) original hydrogen index (HIo) estimated to be approximately 680 mg HC/g TOC; (3) moderate depths of 3.150 m; (4) overpressure distribution in the order of 47–61 MPa, (5) lack of expandable clays in mature areas; and (6) different landing zones for the production of oil, wet gas and dry gas [3, 4, 5, 6, 7, 8].

In addition to the organic geochemical patterns of the Vaca Muerta Formation, petrophysical properties are key factors in hydrocarbon production. Several works correlate laboratory measurements and downhole log information to identify main reservoir properties [9, 10, 11]. However, in the Vaca Muerta Formation reservoir properties and fluid types seem to vary significantly both laterally and vertically suggesting that each interval of interest must be addressed and analyzed separately [11]. Nuclear magnetic resonance (NMR) is a widely used technique to characterize the porosity framework and fluid properties of shale plays due to its non-invasive nature and the possibility of performing in-situ measurements. Recently, the application of low field NMR laboratory measurements to detect both fluid (water and hydrocarbons) and solid-like organic matter components in Vaca Muerta samples was demonstrated, making low field NMR a powerful technique to improve the petrophysical characterization of this unit [12].

The present study examines two wells located in areas where according to regional maturity maps the unit ranges in maturity from the oil window to the gas window [6]. The

* Corresponding author: diana.m.masiero@ypftecnologia.com

main objective of this work is to obtain a workflow that allows a full and integrated petrophysical characterization of the Vaca Muerta Formation. This is achieved by combining different techniques and performing a detailed comparison and integration of the obtained results. The experimental techniques explored in this work include low-field NMR T_1-T_2 maps, organic geochemistry, gas filled porosity, microCT imaging and mineralogical analysis.

2 Data and methods

The present study shows petrophysical, mineralogical and organic geochemistry results integrated with 3D micro-scale reconstructions from rotary sidewall and core samples from two wells: Well A and Well B (Figure 1). The study includes shale samples (13 from Well A, 15 from Well B), but lithologies such as altered tuffs (1 sample, Well A) were also taken into consideration.

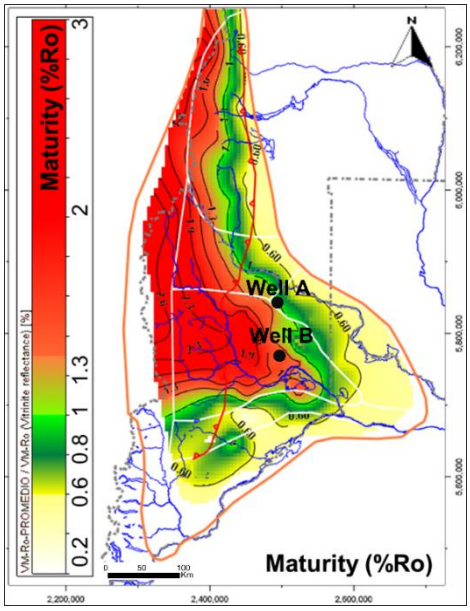

Fig. 1. Vaca Muerta Formation regional maturity map based on Brisson [6], and location of Well A and Well B analyzed in this work.

2.1 Workflow

In Fig. 2 the proposed workflow for characterization of rock samples from the Vaca Muerta formation is presented. This workflow can be applied to any non-conventional rock sample. Special emphasis is made on treating samples "as received" and performing non-destructive measurements to preserve as much sample as possible.

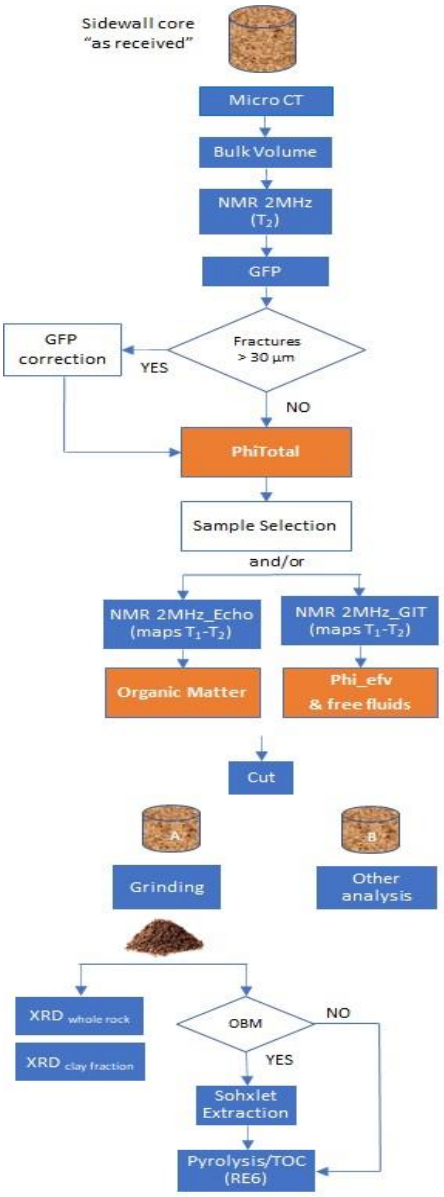

Fig. 2. The integrated workflow used for the analysis of sidewall core samples from Well A and Well B is presented.

2.2 Nuclear Magnetic Resonance (NMR)

NMR measurements were performed at 2.27 MHz with an Oxford Geospec2 analyzer. Samples were measured bulk as received; the average mass of the samples was 40–50 g, approximately. T_2 measurements were carried out with a standard CPMG sequence with echo time 100 µs. This experiment allows to quantify the fluid-filled pore space; total porosity is obtained by adding this value to the GFP porosity (see below).

T_1-T_2 maps were acquired with the SR-FID-ECHO-CPMG sequence introduced by Silletta et al. [12], a scheme that allows to probe the decay of both solid-like and liquid components of shale samples in a single measurement. In this setup, T_1 was encoded with a saturation recovery (SR) sequence with delay time from 21 µs to 390 ms in 50 logarithmic steps. In the T2 dimension, a CPMG pulse sequence was

applied (echo time 200 ms, 500 echoes) sampling one data point at the echo tops. Furthermore, 18 points were sampled during the FID (dwell time 8 ms) before the first 180° pulse of the CPMG; to increase the FID acquisition time a spin echo of t = 200 ms was introduced before the CPMG echo train. The numerical inversion was performed applying the algorithm presented in [13] with exponential kernels in both dimensions. The zones in the T_1-T_2 maps were interpreted as in [12].

2.3 Gas Filled Porosity (GFP)

The empty pore space inside the rock sample is quantified using results from two separate experiments: a Hg pycnometer and GFP. The first, the Hg pycnometer, allows the characterization of the bulk volume. It uses a container filled with Hg whose density is characterized beforehand. Then the sample is fully submersed in the Hg and the change in weight is registered by a scale. The Archimedes method is used to estimate the outer volume of the sample.

The second experiment is known as GFP and is performed using a He Porosimeter from Vinci Technologies. The equipment itself measures grain volume. It has a sample chamber to house the sample and a reference chamber which is loaded with He at 200 psi; both chambers are connected, and the final stabilization pressure is detected. Therefore, the empty space in the sample chamber can be obtained, and by knowing the total volume of the chamber, the grain volume is deduced. It is important to point out that the time it takes the He to occupy the empty pore space will depend directly on the permeability of samples. Thus, lower permeability samples will take longer times than higher permeability ones. A long stabilization time (around 10 minutes) with a strict pressure tolerance (± 0.03 psi) for unconventional rocks is considered. We also repeat the experiment at least three times to make sure that measurements are repeatable.

By combining the bulk volume measurement of the rock with the grain volume, the empty pore space is quantified. This value refers to the part of the porosity that is empty (filled with air) and accessible from the outer surface of the rock.

2.4 X-ray diffraction (XRD)

For mineralogical analysis both bulk rock and clay fraction analysis were done. For bulk rock analysis samples were ground to a fine particle size using a Retsch MM400 mixer mill. X-ray diffraction patterns were collected on random powder specimens using a D8 Advance Bruker X-ray diffractometer (Ni-filtered CuKα, 40 kV, 40mA). A 5–70 deg 2θ range was acquired, with 0.02 deg steps and 0.5 second counting time. Diffraction data were analyzed using DIFFRAC.EVA software for identification of mineralogical phases. Weight percentages of observed phases were calculated using quantitative Rietveld analysis with DIFFRAC.TOPAS.

Determination of clay minerals was performed on the fraction less than 2 μm. Three oriented aggregates were prepared (air-dried, ethylene glycol solvated and calcinated) and their XRD patterns collected in the range of 3–30 deg 2θ with 0.02 deg steps and 0.5 second counting time. Identification of clay mineral phases was based on diagnostic peaks according to Moore and Reynolds [14] and their quantification using NEWMOD program as described in Moore and Reynolds [14].

2.5 Rock Eval programmed pyrolysis

The characterization of organic matter (OM) was performed using a Rock-Eval 6 [15]. Powdered whole rock samples were placed in an oven and first heated to 300°C under an inert atmosphere and then gradually pyrolyzed up to 650°C. After the pyrolysis was completed, samples are gradually heated up to 850°C in the presence of air. The S1 (free hydrocarbons) was not considered since samples were solvent extracted due to the use of oil-based mud during drilling operations. The S2 (hydrocarbons generated by kerogen cracking) and S3 (releasable oxygen) measures allowed to calculate hydrogen and oxygen indices (HI, OI) and estimate kerogen types (from I to IV), using the modified Van Krevelen diagram [16]. The thermal maturity was based on the determination of Tmax [17]. This parameter increases with the maturation degree of the organic matter and was used to obtain a thermal maturity estimation of the analyzed samples.

2.6 X-ray micro–Computed Tomography (microCT)

As a nondestructive technique, X-ray microcomputed tomography provides the required insight into opaque objects eliminating the need of sectioning. Specimens were imaged in a Bruker SkyScan 1173 High Energy desktop microCT at 130 kV and 61 μA with a 0.25 mm brass filter. The cubic voxel size was fixed at 35.72 μm and the samples were rotated around 360° at angular increments of 0.80°. The microCT radiograph projections were reconstructed using NRecon version 1.6.9.8 to obtain an axial slice image dataset. The 8-bit (256 grey values) image dataset was imported into DataViewer version 1.5.0 for visualization. The images obtained provide detailed visualization of the internal fabric and recognition of heterogeneities including fractures [18]. In grayscale images black correspond to air, dark grays to low X-ray absorbing minerals like quartz or feldspars and bright grays to higher X-ray absorbing phases such as calcite or, in white, pyrite. Segmentation and analysis of microCT images allow for the quantification of porosity associated with open fractures (> 30 μm thick) as observed for Well A (Figure 4). With image processing percentage of open fractures, in dark gray, was calculated with respect to the total volume. As pores in the internal structure have sizes lower than the

resolution of the images, they are not considered in the segmentation. Thus, GFP was corrected only to include pores in the internal structure of the rock.

3 Results and Discussion

3.1 Well A

Shale samples are characterized by high present-day TOC contents ranging from 3–7.20% (mean: 4.30%), with maximum values registered in siliciclastic-rich (< 30% of calcite) samples (Table 1). The S2 peak which coincides with the remaining potential of hydrocarbon generation ranges from 2.84–12.75 mgHC/grock (mean: 5.75); whereas the HI shows values between 103–177 mgHC/gTOC (mean: 130). Rock Eval® Tmax values (458–462°C, mean: 460) point to analyzed samples being mature in the late oil window (Fig. 3). As expected, anomalous values of TOC (< 1%) and S2 (< 1 mg/g) were determined in altered tuff levels.

According to whole rock XRD analysis, siliciclastic-rich shales are mainly composed of quartz (22–41%, mean: 31), plagioclase (13–19%, mean: 16), and clay minerals (12–21%, mean: 16) with minor proportions of K-feldspar, pyrite and apatite. On the contrary, carbonate-rich samples show a predominance of calcite (50–60%, mean 53). Mixed carbonate-siliciclastic (30–50% of calcite) shales exhibit variable proportion of quartz (18–25%, mean: 23), plagioclase (9–12%, mean: 11), and clay minerals (9–15%, mean: 11). The composition of the clay fraction does not display vertical differences with illite-smectite (expandable layers < 10%) as the dominant phase.

In some siliciclastic-rich samples, microCT images reveal original depositional features with very thin parallel lamination and organized in lenticular fabrics. Massive fabrics are observed in carbonate-siliciclastic and carbonate-rich samples (Fig. 4). There is no evidence of internal disposition, possibly because the main components are smaller than the resolution achieved. MicroCT was an important tool to resolve the occurrence of fracture porosity, considering they derive from the extraction of samples from the well. In such cases, GFP values were corrected by subtracting the porosity associated with fractures. Due to experimental limitations on the microCT resolution, only fractures greater than 30 µm thick were considered.

The combination of GFP and T_2 measurements yield for shale samples values in the order of 12 – 19 porosity units (pu), with maximum porosities registered in siliciclastic shales (Table 1).

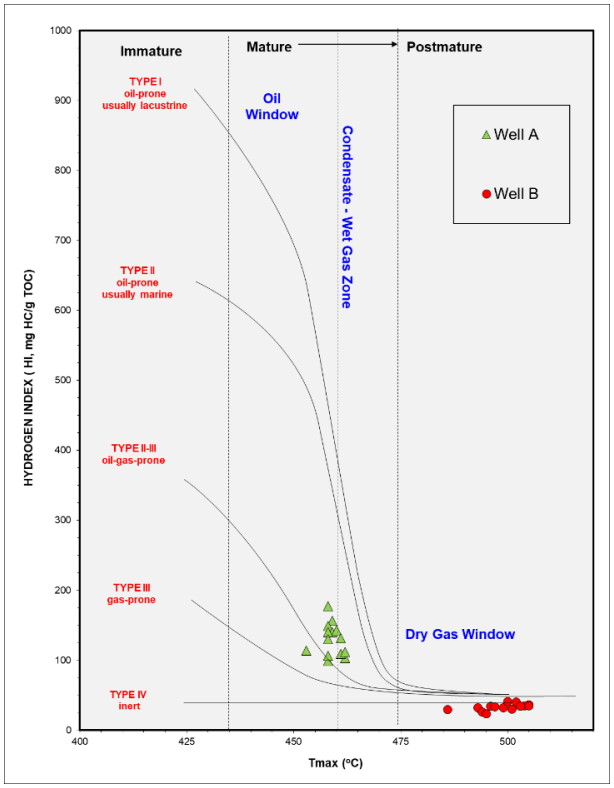

Fig. 3. HI vs. Tmax diagram for the analyzed samples from Well A and Well B (type lines modified from Espitalié et al. [16]).

Table 1. Summary with results for Well A. Minimum, maximum and mean values are presented.

	Siliciclastic shales (n: 5)	Carbonate-siliciclastic shales (n: 3)	Carbonate shales (n: 5)
TOC [%]	3 – 7 (5)	3 – 5 (4)	2 – 4 (3)
Carbonates [%]	15 – 29 (25)	31 – 48 (45)	52 – 61 (57)
Qz + Feld [%]	40 – 62 (49)	31 – 39 (35)	27 – 34 (30)
Clays [%]	12 – 21 (16)	9– 15 (11)	7 – 9 (8)
GFP_AR [pu]	3 – 6 (4)	4 – 6 (5)	3 – 6 (4)
PhiRMN_AR [pu]	10 – 13 (12)	10– 13 (11)	8 – 11 (9)
PhiTotal_AR [pu]	14 – 19 (16)	15 – 17 (16)	12 – 16 (14)

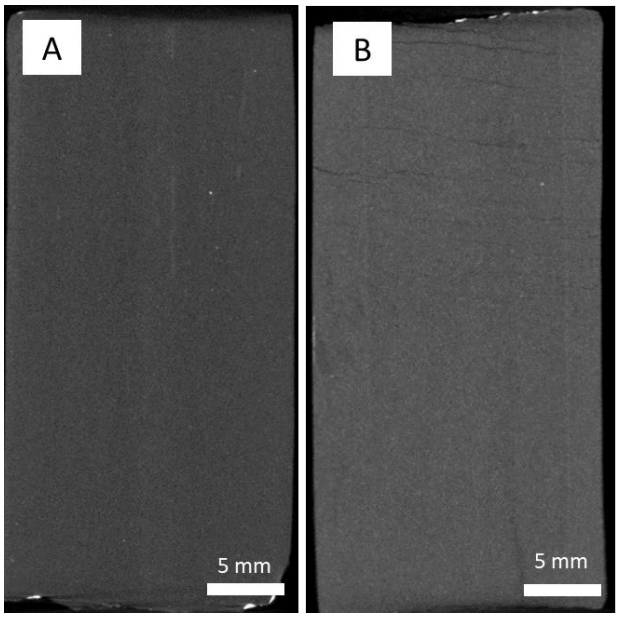

Fig. 4. Examples of microCT images from Well A samples. A and B) Massive aspect observed in carbonate-siliciclastic and carbonate-rich samples.

Further characterization of the components inside the rock was achieved by NMR measurements. Fluid contribution to porosity was obtained from T_2 NMR measurements (Table 1). T_1-T_2 maps give further information on the hydrogen rich components present in the rock. A typical map for Well A can be seen in Fig. 5. The following zone identification is adopted from [12]: zone 1 corresponds to hydroxyl groups present in the inorganic components of shales (clay or other minerals); zone 2 is associated with solid organic matter, kerogen, bitumen and light hydrocarbons inside the kerogen network; zone 3 is attributed to clays; zone 4 is corresponds to moveable hydrocarbons.

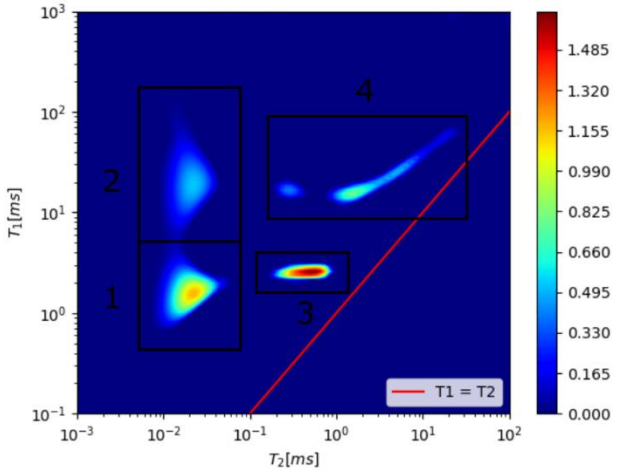

Fig. 5. NMR T_1-T_2 map for a representative sample of Well A. Four zones are clearly marked by black rectangles.

Quantification of NMR signal per zone is performed for each of the 13 samples from Well A. NMR results are integrated with XRD and Rock-Eval measurements. Zone 3 is correlated with clay content from XRD (Fig. 6); zone 2 is correlated with TOC values from Rock Eval pyrolysis (Fig. 7). Both integrations show a very good correlation. This indicates that the three experimental techniques are comparable. Also, since both XRD and Rock-Eval only consider less than 2–3 grams of mass, while NMR is performed on whole rock (approximately 40 grams for Well A samples), the good correlation points to representativity of subsample extraction and homogeneity of the sample.

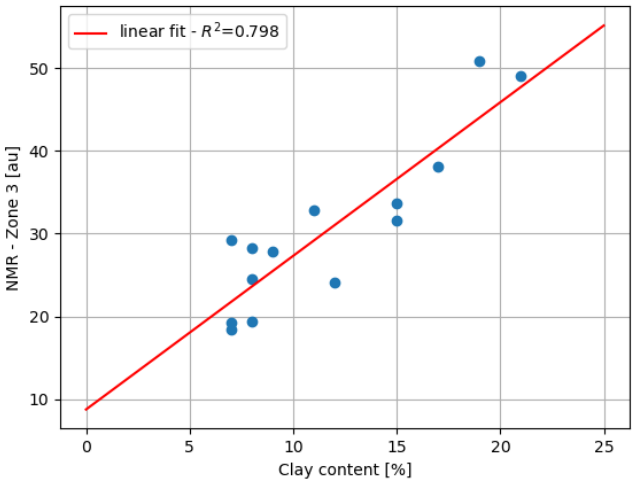

Fig. 6. NMR signal from zone 3 is plotted against clay content in the rock from XRD. A linear fit is performed (red line). R^2 stands for the coefficient of determination of the least-squares.

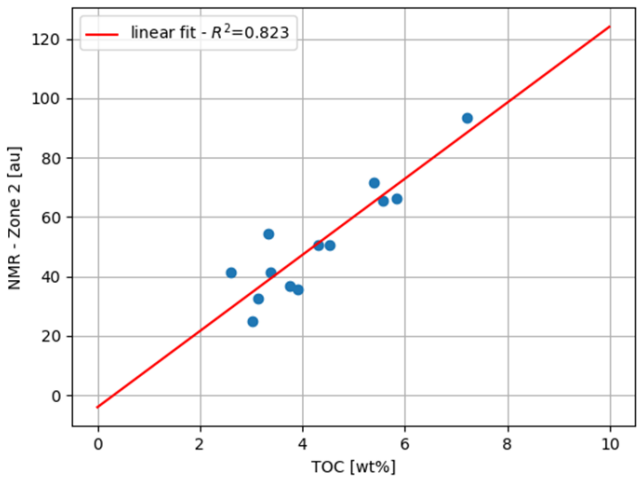

Fig. 7. NMR signal from zone 2 is plotted against TOC value from Rock-Eval pyrolysis. A linear fit is performed (red line). R^2 stands for the coefficient of determination of the least-squares.

3.2 Well B

Shale samples from Well B also show high present day TOC contents (0.72–11.77%, mean: 5.86), with S2 peak ranging from 0.21–4.14 mgHC/grock (mean: 1.93) and HI of 23–40

mgHC/gTOC (mean: 32). Rock Eval® Tmax values (486–506°C, mean: 499) are higher than those presented for Well A, indicating that in the position of Well B the unit reached the wet gas window (Fig. 3).

Based on the adopted compositional scheme, most analyzed samples are siliciclastic-rich (< 30% of calcite) with the highest TOC contents (Table 2). They are composed of quartz (15–37%, mean: 26), plagioclase (9–34%, mean: 20), and clay minerals (18–43%, mean: 28) with minor proportions of K-feldspar, pyrite and apatite. Two samples of the analyzed set correspond to the mixed carbonate-siliciclastic (30–50% of calcite), whereas only one represents the carbonate-rich (> 50% of calcite) shales. However, the latter shows important micro-fractures filled with calcite which impacted in the calculated whole rock composition. Calcite mm-thick micro-fractures were observed under microCT acquisitions as well as interbedded laminae showing compositional and grain size changes (Fig. 8).

According to GFP and T_2 measurements shale samples show porosity values of 10 – 17 pu (Table 2).

Table 2. Summary with results for Well B. Minimum, maximum and mean values are presented.

	Siliciclastic shales (n: 12)	Carbonate-siliciclastic shales (n: 2)	Carbonate shales (n: 1)
TOC [%]	1 – 12 (6)	5– 6	6
Carbonates [%]	12 – 29 (19)	43 – 45	60
Qz + Feld [%]	36 – 53 (46)	41 – 43	27
Clays [%]	18 – 43 (28)	8– 11	10
GFP_AR [pu]	2– 10 (7)	7 – 8	6
PhiRMN_AR [pu]	6 – 10 (7)	5	4,5
PhiTotal_AR [pu]	11 – 17 (14)	12 – 13	10,5

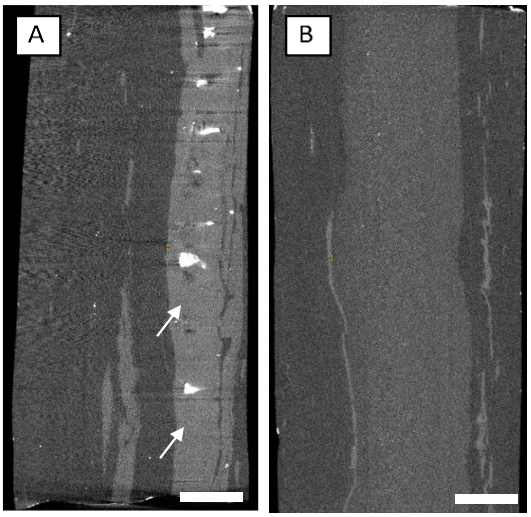

Fig. 8. Examples of microCT images from Well B samples. A) Organic-rich, siliciclastic shale with calcite microfractures (white arrows). B) Siliciclastic shale with internal heterogenies as result of compositional and grain-size changes. Scale bar = 5 mm.

A similar NMR workflow was performed on samples from Well B, where T_2 measurements account for the porosity associated with fluids in the rock, while NMR T_1-T_2 maps allow for component typification. In Fig. 9 a representative T_1-T_2 map for a sample in Well B is shown. Four different zones are marked with black rectangles.

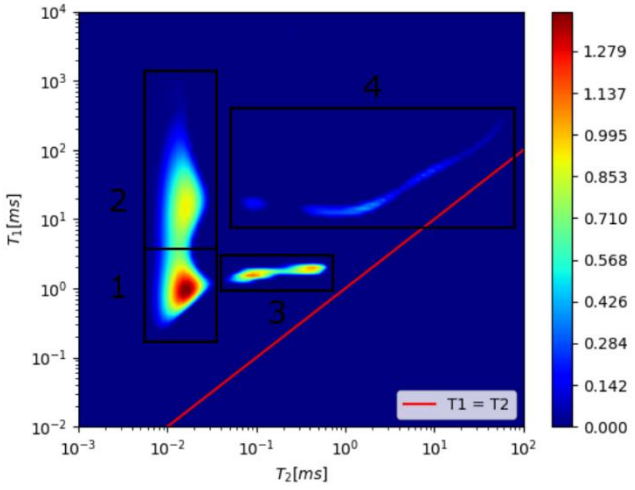

Fig. 9. NMR T_1-T_2 map for a representative sample of Well B. Four zones are clearly marked by black rectangles.

The NMR signal corresponding to each zone is calculated and the results are compared to XRD and Rock-Eval pyrolysis. Zone 3 is compared to clay content (Fig. 10) while zone 2 is compared to TOC (Fig. 11). As in the case of Well A, NMR signal from zone 3 strongly correlates to clay content obtained from XRD analysis. In the case of zone 2 and TOC values, the correlation is not as strong, and the data points show a larger dispersion compared with Well A. We consider that different variables might have controlled the observed uncertainty: (1) Wells represent different maturity window, oil window for Well A and gas window for Well B; (2) the analyzed set for both Wells does not strictly represent the same organic-rich intervals of the Vaca Muerta Formation;

and (3) the internal heterogeneities documented through microCT images. Another possible reason for this discrepancy in correlation could come from the difference in measured mass in Rock-Eval (less than 2–3 grams) and NMR (whole rock, more than 40 grams). Accordingly, further work is necessary to find the cause of the dispersion in values of NMR zone 2 for Well B samples.

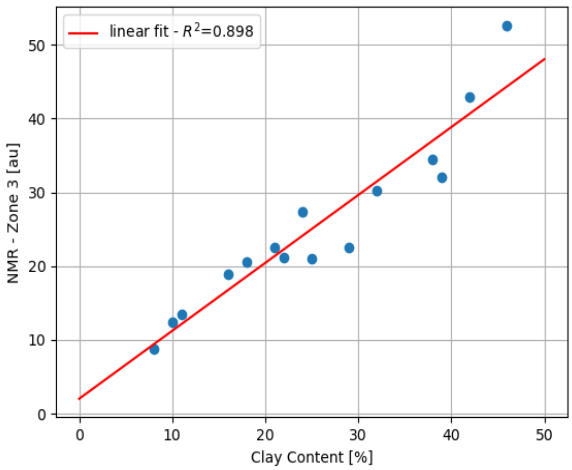

Fig. 10. NMR signal from zone 3 is plotted against clay content in the rock from XRD. A linear fit is performed (red line). R^2 stands for the coefficient of determination of the least-squares.

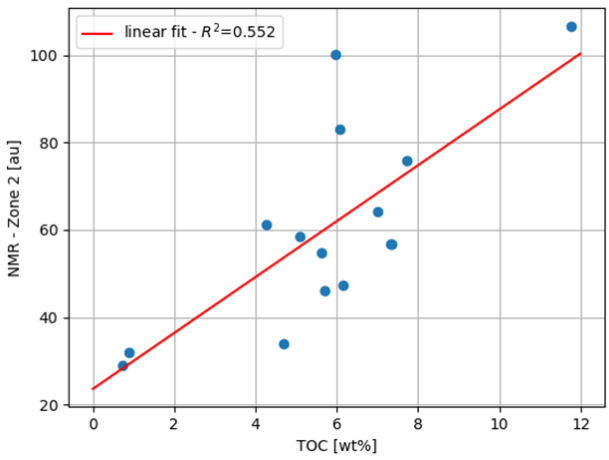

Fig. 11. NMR signal from zone 2 is plotted against TOC value from Rock-Eval pyrolysis. A linear fit is performed (red line). R^2 stands for the coefficient of determination of the least-squares.

4 Conclusions

The present study analyzed samples of the Vaca Muerta Fm based on RMN T_1-T_2 maps at 2 MHz combined with GFP, XRD, Rock-Eval pyrolysis and microCT data with the intent of defining a multi-scale and multidisciplinary petrophysical workflow that can be used for the evaluation of sidewall and core samples at different thermal maturities.

The unit is an heterogenous system independent of the scale of work. GFP and T_2 measurements have shown total porosity values ranging from 10 pu to 19 pu, with maximum porosities recorded in siliciclastic shales (< 30% of calcite). Rock-Eval pyrolysis confirm that a part of the analyzed siliciclastic shales has the largest organic carbon contents.

MicroCT images reveal different types of heterogeneities including open fractures as those recorded in Well A. In such cases, indirect measurements of parameters (e.g., porosity by GFP) do not account for the origin of pores and, for example, do not determine whether the sample is fractured or not. Imaging techniques, such as microCT, together with Digital Rock Analysis (DRA), allow the study of heterogeneities in the rock, as those described in this work, and are of great importance to discriminate open or closed fractures and achieve more reliable porosity measurements.

The presence of heterogeneities as well as other variables, such as the difference in measured mass, might impact in the correlation between NMR and direct rock analysis (e.g., TOC% via pyrolysis Rock Eval). In the future, new measurement strategies can be refined to reliably discern the causes of data dispersion.

This study is published with the permission of YPF, EQUINOR and Y-TEC. We are especially grateful to C. Smal, M. Sánchez, G. Bobrovsky and J. P. Alvarez (Y-TEC) and V. Consoli, D. Ceccon, M. Foster, C. Bernhardt, M. Fasola, I. Brisson and G. Sagasti (YPF) for allowing us to publish the present data.

Special thanks for the technical staff at Y-TEC (J. Juárez, D. Robledo, G. Otegui, J. Acosta, K. Irvicelli, I. Loyza, R. Panno) for the preparation and acquisition of core samples and data analyzed in this study.

References

1. R.L. Kleinberg, W.E. Kenyon, P.P. Mitra, J. Magn. Reson Ser A, **108**, 206-214 (1994)
2. G.R. Coates, L. Xiao, M. Prammer. Nmr Logging, 251, (1999)
3. M. Uliana, L. Legarreta, Journal of Petroleum Geology, **16**, 397–420, (1993)
4. G. Sagasti, M. Foster, D. Hryb, A. Ortiz, V. Lazzari, *Unconventional Resources Technology Conference,* 797-816, (2014)
5. R.F. Dominguez, M. Di Benedetto, *Unconventional Resources Technology Conference*, 5114-5128, (2019)
6. I.E Brisson, M.E. Fasola, H.J. Villar, *Integrated geology of unconventionals: The case of the Vaca Muerta play, Argentina,* AAPG Memoir **121**, 297-328, (2020)
7. J.B. Spacapan, M. Comerio, I. Brisson, E. Rocha, M. Cipollone, J.C. Hidalgo, Basin Research, **33**, 3183-3211 (2021)
8. J.B. Spacapan, M. Comerio, R. Ruiz, E. Rocha, Journal of Petroleum Geology **45**, 219-248, (2022)

9. A. Askenazi, P. Biscayart, M. Cáneva, S. Montenegro, S., M. Moreno, M, Society of Petroleum Engeneers (SPE), (2013)
10. S. Cuervo, E. Lombardo, D. Vallejo, L. Crousse, C. Hernandez, L. Mosse, Unconventional Resources Technology Conference (URTeC), 778-796, (2016)
11. A.C. Ortiz, L. Crousse, C. Bernhardt, D. Vallejo, L. Mosse, Integrated geology of unconventionals: The case of the Vaca Muerta play, Argentina, AAPG Memoir **121**, 329-350, (2020)
12. E.V. Silletta, G.S. Vila, E.A. Domené, M.I. Velasco, Fuel, **312**, 122863, (2022)
13. P. Teal, C. Eccles C., Inverse Probl., **31**, 045010, (2015)
14. D.M. Moore, R.C. Reynolds, *X-ray diffraction and the identification and analysis of clay minerals,* (1989)
15. E. Lafargue, F. Marquis, D. Pillot, Revue de l'institut français du pétrole, **53**, 421-437, (1998)
16. J., Espitalié, G. Deroo, F. Marquis, Revue de l'institut Français du Pétrole, **41**, 73-89, (1986)
17. K.E. Peters, AAPG Bulletin, **70**, 318–329, (1986)
18. M. Comerio, D.E. Fernández, N. Rendtorff, M. Cipollone, P.E. Zalba, P.J. Pazos, AAPG Bulletin, **104**, 1679-1705, (2020)